^{23}Na Nuclear Spin-Lattice Relaxation Studies of $Na_2Ni_2TeO_6$

Yutaka ITOH*

Department of Physics, Graduate School of Science, Kyoto Sangyo University, Kyoto 603-8555, Japan

We report on ^{23}Na NMR studies of the honeycomb lattice antiferromagnet $Na_2Ni_2TeO_6$ by ^{23}Na nuclear spin-echo techniques. The ^{23}Na nuclear spin-lattice relaxation rate $1/^{23}T_1$ exhibits critical divergence near the Néel temperature T_N = 26 K, a narrow critical region, and the critical exponent w = 0.34 in $1/^{23}T_1 \propto (T/T_N - 1)^{-w}$ for $Na_2Ni_2TeO_6$, and T_N = 18 K for $Na_2(Ni_{0.5}Cu_{0.5})_2TeO_6$. Although the uniform magnetic susceptibility of $Na_2Ni_2TeO_6$ exhibits a broad maximum at 35 K, which is the characteristic of low-dimensional spin systems, the NMR results indicate a three-dimensional critical phenomenon near the Néel temperature.

1. Introduction

$Na_2Ni_2TeO_6$ is a quasi-two-dimensional honeycomb lattice antiferromagnet.[1–3] The crystal structure of $Na_2Ni_2TeO_6$ consists of the stacking of Na and (Ni/Te)O_6 layers ($P6_3/mcm$).[2,3] The Néel temperature T_N of ≈ 27 K was estimated from measurements of specific heat and the derivative of uniform magnetic susceptibility.[3] The magnetic susceptibility takes a broad maximum at 34 K.[2,3] The Weiss temperature θ of − 32 K and the superexchange interaction J/k_B of − 45 K were estimated from the analysis of a Curie-Weiss law fit and a high-temperature series expansion.[3] Although the Ni^{2+} ion must carry the local moment $S = 1$ on the honeycomb lattice, the large effective moment $\mu_{\rm eff}$ of $3.446\mu_B$ could not be explained by the spin $S = 1$ with a g-factor of 2 .[3] The g-factor must be larger than 2,[2] or a Ni^{3+} ion and the intermediate state might be realized because of the tunable valences of Te^{4+} and Te^{6+}.[3]

Spin frustration effects on a honeycomb lattice have renewed our interest since the discovery of a possible spin liquid state in a spin-3/2 antiferromagnet.[4] Various magnetic ground states compete with each other on the honeycomb lattice.[5]

In this paper, we report on ^{23}Na NMR studies of $Na_2Ni_2TeO_6$ and $Na_2(Ni_{0.5}Cu_{0.5})_2TeO_6$ polycrystalline samples. $Na_2(Ni_{0.5}Cu_{0.5})_2TeO_6$ still belongs to the same space group $P6_3/mcm$ as $Na_2Ni_2TeO_6$.[2,6] For the Cu substitution, we expected a possible enhancement of quantum effects from $S = 1$ to 1/2. Since the solubility limit in the honeycomb lattice $Na_2(Ni_{1-x}Cu_x)_2TeO_6$ is about $x = 0.6$,[6] we selected the half Cu-substituted sample being away from the phase boundary. We observed a three-dimensional critical phenomenon in the ^{23}Na nuclear spin-lattice relaxation rate $1/^{23}T_1$ near T_N = 26 K for $Na_2Ni_2TeO_6$ and T_N = 18 K for $Na_2(Ni_{0.5}Cu_{0.5})_2TeO_6$. The broad maximum of uniform magnetic susceptibility is not the onset of magnetic long-range ordering. In the antiferromagnetic state of $Na_2Ni_2TeO_6$, we observed $1/^{23}T_1 \propto T^3$, which indicates conventional spin-wave scattering.

2. Experimental Procedure

Powder samples of $Na_2Ni_2TeO_6$ were synthesized by a conventional solid-state reaction method. Appropriate amounts of NiO, TeO_6 and Na_2CO_3 were mixed, palletized, and fired 3 times at 800 − 860 °C and finally at 900 °C for 24 h in air. The products were confirmed to be in a single phase from measurements of powder X-ray diffraction patterns. Magnetic susceptibility χ at 1.0 T was measured using a superconducting quantum interference device (SQUID) magnetometer. Powder samples of $Na_2(Ni_{0.5}Cu_{0.5})_2TeO_6$ were previously synthesized and characterized.[6]

A phase-coherent-type pulsed spectrometer was utilized for the ^{23}Na NMR (nuclear spin I = 3/2) experiments at an external magnetic field of 7.4847 T. The NMR frequency spectra were obtained from Fourier transformation of the ^{23}Na nuclear spin-echoes. The ^{23}Na nuclear spin-lattice relaxation curves $^{23}p(t) = 1 - E(t)/E(\infty)$ (recovery curves) were obtained by an inversion recovery technique as a function of time t after an inversion pulse, where the nuclear spin-echoes $E(t)$, $E(\infty)[\equiv E(10T_1)]$ and t were recorded.

3. Experimental Results and Discussion

3.1 Uniform magnetic susceptibility

Figure 1 shows the uniform magnetic susceptibility χ of $Na_2Ni_2TeO_6$ and $Na_2(Ni_{0.5}Cu_{0.5})_2TeO_6$. The solid curves are the results from least-squares fits by the Curie-Weiss law. We estimated the Weiss temperature θ = − 27 K and the effective

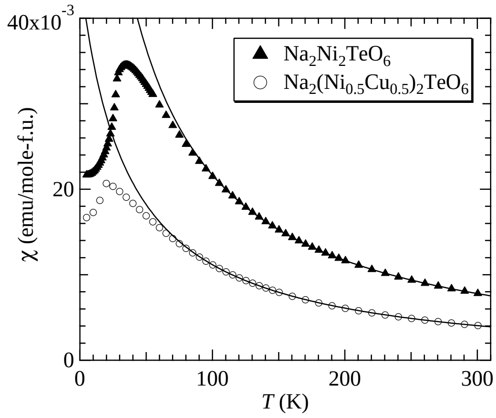

Fig. 1. Uniform magnetic susceptibility χ of $Na_2Ni_2TeO_6$ and $Na_2(Ni_{0.5}Cu_{0.5})_2TeO_6$. Solid curves are the results from least-squares fitting using the Curie-Weiss law.

*yitoh@cc.kyoto-su.ac.jp

moment $\mu_{\text{eff}} = 3.4\mu_B$ for $Na_2Ni_2TeO_6$, which are in agreement with a previous report,[3] and $\theta = -35$ K and $\mu_{\text{eff}} = 2.5\mu_B$ for $Na_2(Ni_{0.5}Cu_{0.5})_2TeO_6$. If the g-factor is 2, then $S = 1$ and 1/2 lead to $\mu_{\text{eff}} = 2.83\mu_B$ and $1.73\mu_B$, respectively. χ deviates below about 100 K from the Curie-Weiss law and takes a broad maximum at 35 K in $Na_2Ni_2TeO_6$. χ drops below about 20 K in $Na_2(Ni_{0.5}Cu_{0.5})_2TeO_6$.

3.2 NMR spectrum and recovery curves

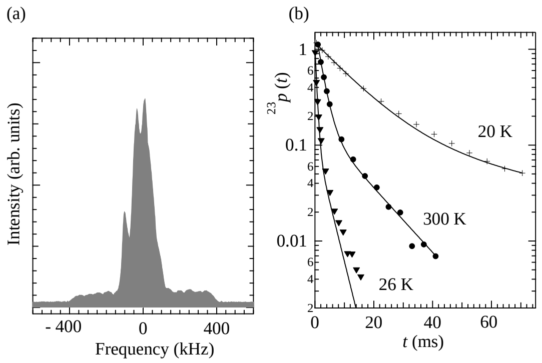

Fig. 2. (a) Fourier-transformed ^{23}Na NMR spectrum at 84.670 MHz and 300 K. (b) ^{23}Na nuclear spin-lattice relaxation curves $^{23}p(t)$ at a central frequency. Solid curves are the results from least-squares fitting using Eq. (1).

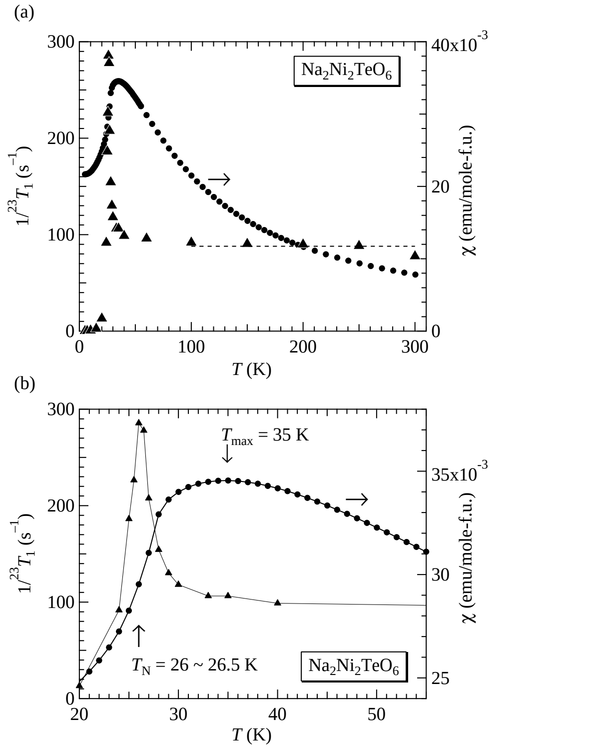

Fig. 3. (a) $1/^{23}T_1$ and uniform magnetic susceptibility χ against temperature. $1/^{23}T_1$ shows a critical divergence near $T_N = 26 - 26.5$ K and levels off above about 100 K. The broken line indicates $1/^{23}T_{1\infty} = 88$ s^{-1}. (b) $1/^{23}T_1$ and χ against temperature in enlarged scales. Solid curves are visual guides.

Figure 2(a) shows the Fourier-transformed spectrum of ^{23}Na spin-echoes at a Larmor frequency of 84.670 MHz and at 300 K. The central transition line $Iz = 1/2 \leftrightarrow -1/2$ is affected by a nuclear quadrupole interaction.[7] The linewidth is about 150 kHz. The precise value of the Knight shift could not be determined in the present studies.

Figure 2(b) shows the recovery curves $^{23}p(t)$ at various temperatures. The solid curves are the results from least-squares fitting using a theoretical multiexponential function for a central transition line ($I_z = 1/2 \leftrightarrow -1/2$),

$$^{23}p(t) = p(0)\{0.1e^{-t/^{23}T_1} + 0.9e^{-6t/^{23}T_1}\}, \tag{1}$$

where $p(0)$ and the ^{23}Na nuclear spin-lattice relaxation time $^{23}T_1$ are fit parameters. The theoretical function of Eq. (1) well reproduces the experimental recovery data. Thus, the assignment of the exciting spectrum to the central transition line is also justified *a posteriori*.

3.3 $Na_2Ni_2TeO_6$

Figures 3(a) and 3(b) show $1/^{23}T_1$ and the uniform magnetic susceptibility χ against temperature. $1/^{23}T_1$ takes $1/^{23}T_{1\infty} = 88$ s^{-1} above about 100 K and shows a divergence at 26 − 26.5 K, which can be assigned to the Néel temperature T_N. Thus, the broad maximum of the magnetic susceptibility χ at 35 K is not due to the antiferromagnetic long-range ordering but due to a low-dimensional short-range correlation developing on the honeycomb lattice antiferromagnets.[8] The result is consistent with the specific heat measurements.[3]

Figure 4(a) shows $1/^{23}T_1$ against temperature and the result (the solid curve) from least-squares fitting using

$$\frac{1}{^{23}T_1} = \frac{C}{^{23}T_{1\infty}} \frac{1}{|T/T_N - 1|^w}, \tag{2}$$

where the constant C, the Néel temperature T_N, and the critical exponent w are fit parameters. The fitting results were T_N = 26.24 K and $w = 0.34$.

A mean field theory for a three-dimensional isotropic Heisenberg antiferromagnet gives $w = 1/2$.[9] A dynamic scaling theory gives $w = 1/3$ for a three-dimensional isotropic Heisenberg model[10] and $w = 2/3$ for a three-dimensional uniaxial anisotropic Heisenberg model.[11] The exponent of w = 0.34 indicates that $Na_2Ni_2TeO_6$ in the critical region is described by a three-dimensional dynamical spin susceptibility. In passing, CuO exhibits a similar $w = 0.33$, a broad maximum in χ at 540 K, and $T_N = 230$ K.[12]

Figure 4(b) shows log-log plots of normalized $(1/^{23}T_1)/(1/^{23}T_{1\infty})$ against the reduced temperature $|T - T_N|/T_N$. The solid line indicates the result from a least-squares fit by Eq. (2).

The onset of increase in the NMR relaxation rate near T_N empirically categorizes critical regions. The region of $|T - T_N|/T_N \leq 10$ has been assigned to the renormalized classical regime with a divergent magnetic correlation length toward $T = 0$ K.[13] The region of $|T - T_N|/T_N \leq 1.0$ has been assigned to the three-dimensional critical regime with a divergent magnetic correlation length toward T_N. Thus, the narrow critical region of $|T - T_N|/T_N \leq 1$ also empirically categorizes $Na_2Ni_2TeO_6$ to the three-dimensional critical regime.

At high temperatures of $T \gg J$, the spin system is in the exchange narrowing limit. Then, $1/^{23}T_1$ is expressed as

$$\frac{1}{^{23}T_{1\infty}} = \sqrt{2\pi}\frac{S(S+1)}{3}\frac{z_n(^{23}\gamma_n A)^2}{\omega_{ex}}, \tag{3}$$

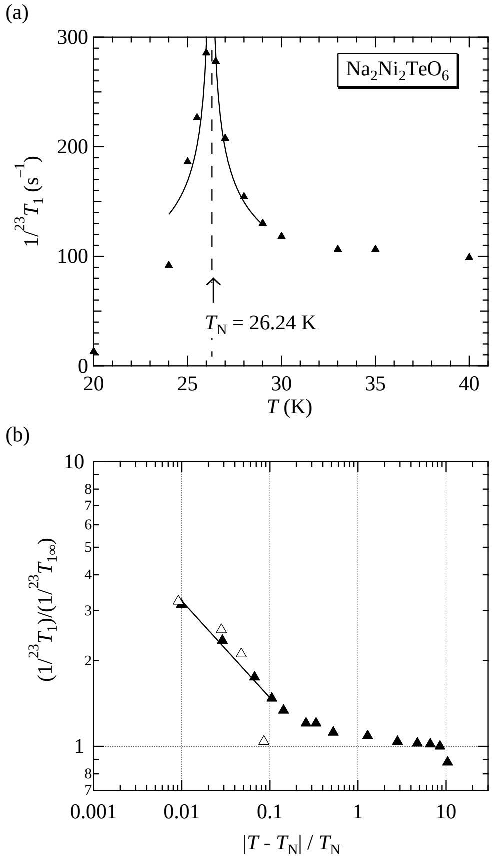

Fig. 4. (a) $1/^{23}T_1$ against temperature. The solid curve is the result from least-squares fitting using Eq. (2). The Néel temperature and the critical exponent were estimated to be T_N = 26.24 K and w = 0.34, respectively. (b) Log-log plots of normalized $(1/^{23}T_1)/(1/^{23}T_{1\infty})$ against reduced temperature $|T - T_N|/T_N$. Closed and open triangles indicate $1/^{23}T_1$ above and below T_N, respectively. The solid line indicates the result from least-squares fitting using Eq. (2).

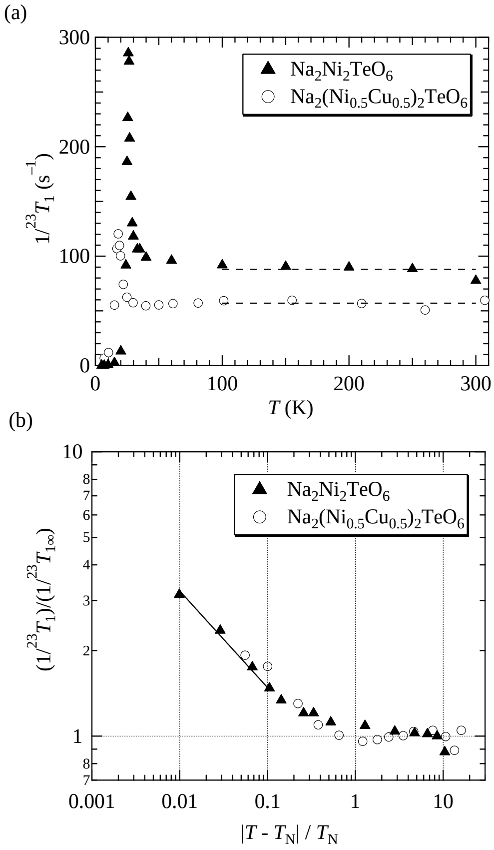

Fig. 5. (a) $1/^{23}T_1$ against temperature for $Na_2Ni_2TeO_6$ and $Na_2(Ni_{0.5}Cu_{0.5})_2TeO_6$. The broken lines indicate $1/^{23}T_{1\infty}$ = 88 and 57 s^{-1}. (b) Log-log plots of normalized $(1/^{23}T_1)/(1/^{23}T_{1\infty})$ against reduced temperature $|T - T_N|/T_N$ for $Na_2Ni_2TeO_6$ (T_N = 26.24 K) and $Na_2(Ni_{0.5}Cu_{0.5})_2TeO_6$ (T_N = 18 K). The solid line is Eq. (2) with the critical exponent w = 0.34.

$$\omega_{ex}{}^2 = \frac{2}{3}S(S+1)z\left(\frac{J}{\hbar}\right)^2, \tag{4}$$

where $^{23}\gamma_n/2\pi$ = 11.262 MHz/T is the ^{23}Na nuclear gyromagnetic ratio, A is the hyperfine coupling constant, and ω_{ex} is the exchange frequency.[14] z_n is the number of Ni ions near a ^{23}Na nuclear. z is the number of nearest-neighbor Ni ions. Assuming J = 45 K,[3] $S = 1$, and $z = 3$, we obtained $\omega_{ex} = 12 \times 10^{12}$ s^{-1}. From Eq. (3) with $1/^{23}T_{1\infty}$ = 88 s^{-1}, we derived the hyperfine coupling constant $A = 2.0$ kOe/μ_B, which is nearly the same as that of $Na_3Cu_2SbO_6$.[15]

3.4 $Na_2(Ni_{0.5}Cu_{0.5})_2TeO_6$

Figure 5(a) shows $1/^{23}T_1$ against temperature for $Na_2Ni_2TeO_6$ and $Na_2(Ni_{0.5}Cu_{0.5})_2TeO_6$. For the half substitution of Cu for Ni, $1/^{23}T_{1\infty}$ and T_N decrease to 57 s^{-1} and 18 K, respectively. Extrapolating linearly T_N with ΔT_N = - 8 K per half Cu to full Cu substitution, one may infer T_N = 10 K of a hypothetical spin-1/2 honeycomb lattice " $Na_2Cu_2TeO_6$," although the actual $Na_2Cu_2TeO_6$ is known to be monoclinic and an alternating spin chain system.[16,17]

Figure 5(b) shows log-log plots of normalized $(1/^{23}T_1)/(1/^{23}T_{1\infty})$ against the reduced temperature $|T - T_N|/T_N$ for $Na_2Ni_2TeO_6$ (T_N = 26.24 K) and $Na_2(Ni_{0.5}Cu_{0.5})_2TeO_6$ (T_N = 18 K). The solid line indicates Eq. (2) with the critical exponent w of 0.34. The critical region of $Na_2(Ni_{0.5}Cu_{0.5})_2TeO_6$ is still narrow, the same as that of $Na_2Ni_2TeO_6$. Simply, T_N decreases. No dimensional crossover is observed.

3.5 Below T_N

Figure 6 shows log-log plots of $1/^{23}T_1$ against temperature for $Na_2Ni_2TeO_6$ and $Na_2(Ni_{0.5}Cu_{0.5})_2TeO_6$. With cooling below T_N, $1/^{23}T_1$ rapidly decreases. The broken line indicates a T^3 function as a visual guide. In conventional antiferromagnetic states, the nuclear spin transitions are caused by Raman scattering and three-magnon scattering.[18] Then, $1/T_1$ is expressed as

$$\frac{1}{T_1} \propto \left(\frac{T}{T_N}\right)^3 \tag{5}$$

in the temperature range of $T_N > T \gg T_{AE}$, where T_{AE} corresponds to an energy gap in the spin wave spectrum.[18] The energy gap is due to a crystalline anisotropy field. The rapid drop of $1/^{23}T_1$ below T_N results from the suppression of low-energy excitations by the energy gap. Below T_{AE}, an activation-type temperature dependence should be observed in $1/T_1$. Since no activation behavior was observed down to 5 K, one may estimate $T_{AE} < 5$ K.

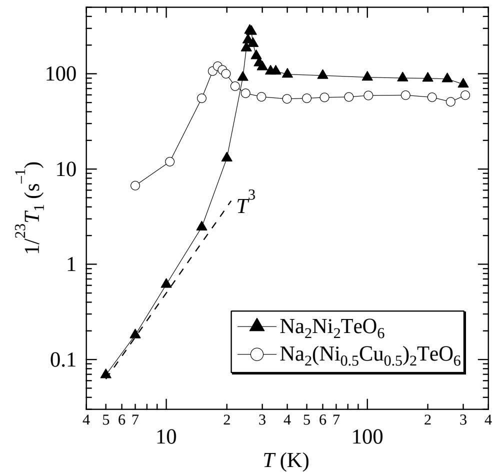

Fig. 6. Log-log plots of $1/^{23}T_1$ against temperature for $Na_2Ni_2TeO_6$ and $Na_2(Ni_{0.5}Cu_{0.5})_2TeO_6$. A broken line indicates a function of Eq. (5). The solid curves are visual guides.

4. Conclusions

In conclusion, we found the three-dimensional critical phenomenon near $T_N = 26$ K for $Na_2Ni_2TeO_6$ and $T_N = 18$ K for $Na_2(Ni_{0.5}Cu_{0.5})_2TeO_6$ from measurements of the ^{23}Na nuclear spin-lattice relaxation rate $1/^{23}T_1$. We have analyzed the NMR results assuming Ni^{2+} with $S = 1$ and obtained sound values of parameters for $Na_2Ni_2TeO_6$. We attribute the deviation from the Curie-Weiss law and the broad maximum of uniform magnetic susceptibility to two-dimensional spin-spin correlation on a honeycomb lattice.

The author thanks M. Isobe (Max Planck Institute) for X-ray diffraction measurements and K. Morimoto, C. Michioka, and K. Yoshimura (Kyoto University) for the sample preparation and characterization at the preliminary stage.

1) Y. Miura, R. Hirai, Y. Kobayashi, and M. Sato, J. Phys. Soc. Jpn. **75**, 084707 (2006).
2) R. Berthelot, W. Schmidt, A. W. Sleight, and M. A. Subramanian, J. Solid State Chem. **196**, 225 (2012).
3) R. Sankar, I. P. Muthuselvam, G. J. Shu, W. T. Chen, S. K. Karna, R. Jayavel, and F. C. Chou, CrystEngComm. **16**, 10791 (2014).
4) O. Smirnova, M. Azuma, N. Kumada, Y. Kusano, M. Matsuda, Y. Shimakawa, T. Takei, Y. Yonesaki, and N. Kinomura, J. Am. Chem. Soc. **131**, 8313 (2009).
5) J. B. Fouet, P. Sindzingre, and C. Lhuillier, Eur. Phys. J. B **20**, 241 (2001).
6) K. Morimoto, Y. Itoh, C. Michioka, M. Kato, and K. Yoshimura, J. Magn. Magn. Mater. **310**, 1254 (2007). $Na_2(Ni_{1-x}Cu_x)_2TeO_6$ with $0 \leq x \leq 0.60$ belongs to the space group $P6_3/mcm$, while $Na_2(Cu_{1-x}Ni_x)_2TeO_6$ with $0 \leq x \leq 0.05$ belongs to the space group $C2/m$ (unpublished works).
7) A. Abragam, *Principles of Nuclear Magnetism* (Oxford University Press, Oxford, 1961).
8) N. Onishi, K. Oka, M. Azuma, Y. Shimakawa, Y. Motome, T. Taniguchi, M. Hiraishi, M. Miyazaki, T. Masuda, A. Koda, K. M. Kojima, and R. Kadono, Phys. Rev. B **85**, 184412 (2012).
9) T. Moriya, Prog. Theor. Phys. **28**, 371 (1962).
10) B. I. Halperin and P. C. Hohenberg, Phys. Rev. Lett. **19**, 700 (1967).
11) E. Riedel and F. Wegner, Phys. Rev. Lett. **24**, 730 (1970).
12) Y. Itoh, T. Imai, T. Shimizu, T. Tsuda, H. Yasuoka, and Y. Ueda, J. Phys. Soc. Jpn. **59**, 1143 (1990).
13) Y. Itoh, C. Michioka, K. Yoshimura, K. Nakajima, and H. Sato, J. Phys. Soc. Jpn. **78**, 023705 (2009).
14) T. Moriya, Prog. Theor. Phys. **16**, 641 (1956).
15) C. N. Kuo, T. S. Jian, and C. S. Lue, J. Alloys Compd. **531**, 1 (2012).
16) J. Xu, A. Assoud, N. Soheilnia, S. Derakhshan, H. L. Cuthbert, J. E. Greedan, M. H. Whangbo, and H. Kleinke, Inorg. Chem. **44**, 5042 (2005).
17) K. Morimoto, Y. Itoh, K. Yoshimura, M. Kato, and K. Hirota, J. Phys. Soc. Jpn. **75**, 083709 (2006).
18) D. Beeman and P. Pincus, Phys. Rev. **166**, 359 (1968).